Biochemical and Biophysical Research Communications 450 (2014) 1104–1109

Contents lists available at ScienceDirect

Biochemical and Biophysical Research Communications

journal homepage: www.elsevier.com/locate/ybbrc

An inhibitor of Na^+/Ca^{2+} exchange blocks activation of insect olfactory receptors

Y. Bobkov [a,*], E. Corey [a], B. Ache [a,b]

[a] Whitney Laboratory, Center for Smell and Taste, McKnight Brain Institute, United States
[b] Depts. of Biology and Neuroscience, Univ. of Florida, Gainesville, FL 32610, United States

ARTICLE INFO

Article history:
Received 18 June 2014
Available online 1 July 2014

Keywords:
Mosquito olfactory receptor
Ionotropic receptor
Sodium calcium exchanger
Inhibition

ABSTRACT

Earlier we showed that the Na^+/Ca^{2+} exchanger inhibitor, KB-R7943, potently blocks the odor-evoked activity of lobster olfactory receptor neurons. Here we extend that finding to recombinant mosquito olfactory receptors stably expressed in HEK cells. Using whole-cell and outside-out patch clamping and calcium imaging, we demonstrate that KB-R7943 blocks both the odorant-gated current and the odorant-evoked calcium signal from two different OR complexes from the malaria vector mosquito, *Anopheles gambiae*, AgOr48 + AgOrco and AgOr65 + AgOrco. Both heteromeric and homomeric (Orco alone) OR complexes were susceptible to KB-R7943 blockade when activated by VUAA1, an agonist that targets the Orco channel subunit, suggesting the Orco subunit may be the target of the drug's action. KB-R7943 represents a valuable tool to further investigate the functional properties of arthropod olfactory receptors and raises the interesting specter that activation of these ionotropic receptors is directly or indirectly linked to a Na^+/Ca^{2+} exchanger, thereby providing a template for drug design potentially allowing improved control of insect pests and disease vectors.

1. Introduction

Unlike vertebrates which use G protein-coupled receptor-based chemosensory transduction, arthropods use ionotropic receptors, including olfactory receptors (Ors), gustatory receptors (GRs) and variant ionotropic glutamate receptors (IRs) [1–6]. ORs and GRs are both seven transmembrane odorant-gated ion channels, while IRs are predicted to be structurally similar to traditional ionotropic glutamate receptors with a bipartite ligand-binding domain separated by an ion pore forming region [5]. Despite their overall structural differences, ORs and IRs both form heteromultimeric complexes composed of a broadly expressed coreceptor and one or more additional subunits that determine the odorant specificity [1,2,7].

In addition to sharing supramolecular organization principles, ORs and IRs share common pharmacology in that both chemoreceptor families are sensitive to ruthenium red, amiloride and/or amiloride derivatives (ADs) [8,1,6,9,10]. Common susceptibility to these pharmacological agents suggests structural similarity of functional elements of the receptor complexes, e.g., the channel pore structure, and/or functional interaction with one or more ubiquitously expressed receptor-associated proteins. Specifically, the reported sensitivity to ADs, especially to pyrazine derivatives of amiloride, and the relative insensitivity to amiloride itself (e.g. [11,12] see [13,14] for review) potentially implicates the involvement of a Na^+/Ca^{2+} exchanger in the activation of ORs and IRs. Further, we previously found that KB-R7943, a compound initially introduced as a Na^+/Ca^{2+} exchange inhibitor [15,16], potently blocks the odor-evoked activity of lobster olfactory receptor neurons [17] which express IRs [18,19]. Based on the common susceptibility of ORs and IRs to other compounds, we explored the possibility that KB-R7943 would also block the activation of insect ORs.

Here we demonstrate that KB-R7943 blocks both the odorant-gated current and the odorant-evoked calcium signal from two different OR complexes from the malaria vector mosquito, *Anopheles gambiae*, AgOr48 + AgOrco and AgOr65 + AgOrco. Both heteromeric and homomeric (Orco alone) OR complexes were susceptible to KB-R7943 blockade when activated by VUAA1, an agonist that targets the Orco channel subunit [7], suggesting the Orco subunit may be the target of the drug's action. KB-R7943 represents a valuable tool to further investigate the functional properties of arthropod ORs and raises the interesting specter that activation of arthropod chemosensory receptors, both ORs and IRs, is directly or indirectly linked to a Na^+/Ca^{2+} exchanger.

* Corresponding author. Address: The Whitney Laboratory for Marine Bioscience, University of Florida, 9505 Ocean Shore Blvd., St. Augustine, FL 32080, United States. Fax: +1 (904) 461 4008.
E-mail address: bobkov@whitney.ufl.edu (Y. Bobkov).

http://dx.doi.org/10.1016/j.bbrc.2014.06.120
0006-291X/

2. Materials and methods

2.1. Heterologous expression

The generation and use of OR-expressing HEK293T cell lines have been previously described [20]. Cells were incubated with 0.3 μg/mL tetracycline for 16 h before the assay to induce OR expression.

2.2. Electrophysiology, calcium imaging and data analysis

AgOR channel activity was investigated using patch clamp recording in different configurations. The whole-cell and channel unitary currents were measured with an 200B patch-clamp amplifier (Molecular Devices, Sunnyvale, CA, USA) and a digital interface (Digidata 1320A, Molecular Devices, Sunnyvale, CA, USA), lowpass filtered at 5 kHz, sampled at 2–20 kHz and in most cases digitally filtered at 1–1.4 kHz. Analysis of the data was carried out using pCLAMP 10 software (Molecular Devices, Sunnyvale, CA, USA) and SigmaPlot 11 (Systat Software Inc., San Jose, CA, USA). Currents were studied at a holding potential of −50 to −40 mV unless otherwise specified. The polarity of the currents/voltages is presented relative to intracellular membrane surface. Patch pipettes were fabricated from borosilicate capillary glass (BF150-86-10, Sutter Instrument, CA, USA) using a Flaming-Brown micropipette puller (P-87, Sutter Instrument, CA, USA). Bath solution change was performed using a rapid solution changer with a modified tube holder, RSC-200 (Bio-Logic – Science Instruments, Claix, France). Data were recorded under continuous perfusion with the solution of interest. The following modification of the Hill equation was used to fit the experimental data for KB dependent channel inhibition, $I = 1 - I_{max} * [KB]^h / ([KB]_{1/2}{}^h + [KB]^h)$, where I are the normalized current values, [KB] is the antagonist concentration, $[KB]_{1/2}$ is the half-effective concentration, and h is the cooperativity coefficient. Whole-cell current–voltage characteristics were generated using series of 15-ms step at −100 mV followed by a 150-ms voltage ramp (linear change in voltage ~0.67 mV/ms) from −100 mV to +100 mV were applied from a holding potential of −50 to −40 mV. The interval between sweep starts was 1 s. The data are presented as the mean ± SE of n observations. All recordings were performed at room temperature (~20–21 °C).

2.3. Solutions and chemicals

The standard extracellular NaCl140mM solution contained (mM): 140 NaCl; 1–2 $CaCl_2$; 0–1 $MgCl_2$; 5 KCl; 10 Hepes. The standard intracellular Na140 mM low calcium solution contained (mM): 140 NaCl; 1–2 EGTA; 10 Hepes. Odorants, δ-decalactone and Eugenol were purchased from Sigma (SAFC 30396PH) and Aldrich (05405JH) and prepared right before experiments as stock solutions 500 mM in dimethyl sulfoxide (DMSO) prior their dilution to different working concentrations. KB-R7943 (Carbamimidothioic acid, 2-[4-[(4-nitrophenyl)methoxy]phenyl]-ethyl ester, methanesulfonate (1:1); CAS Registry Number: 182004-65-5, SciFinder, Fig. 1) was obtained from Tocris, Inc. Drug was dissolved in DMSO to give 100–200 mM stock solutions. The pH of solutions was adjusted with NaOH or Trizma base (Sigma–Aldrich, St. Louis, MO, USA) to 7.3–7.4. VUAA1 (Acetamide, *N*-(4-ethylphenyl)-2-[[4-ethyl-5-(3-pyridinyl)-4H-1,2,4-triazol-3-yl]thio]-; CAS Registry Number: 525582-84-7, SciFinder) was provided by Dr. Zwiebel laboratory. All inorganic salts were purchased from Fisher Scientific (Pittsburgh, PA, USA). All organic compounds were obtained from Sigma–Aldrich.

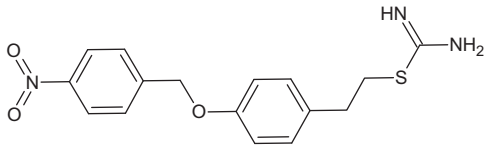

Fig. 1. Chemical structure of KB-R7943.

3. Results and discussion

All AgOR48 + AgOrco-expressing HEK293T cells responded to the cognate odorant δ-decalactone by generating a graded inward current to the maximum stimulus intensity (100 μM) from −34 to −1,721 pA, with a mean amplitude of −413.5 ± 29.5 pA (n = 73, Fig. 2A). Similarly, all AgOR65 + AgOrco-expressing cells responded to the cognate odorant eugenol (100 μM) by generating an inward current from −19 to −934 pA, with a mean amplitude of −212 ± 29pA across 47 cells tested (Fig. 2B). In both instances the appropriate non-cognate odorants, eugenol and δ-decalactone, failed to evoke inward currents, suggesting that activation of respective OR complexes by their cognate odorant was highly specific and providing a control for non-specific activation of the cells by the odorants, the vehicle, and/or the method of stimulus application. In some cases, we used a mixture of eugenol (100 μM) and δ-decalactone (100 μM) to stimulate the cells. While there is evidence of multimodal functioning (ionotropic and metabotropic modes) for at least some ORs [2,21–24], the rapid kinetics and stability of the responses in the whole cell recording mode is consistent with the ionotropic nature of the receptors proposed in the seminal studies [1,2] and later confirmed for a variety of ORs from different insect species (e.g., [7,25,26]).

We tested for AgOR/Orco sensitivity to the Na^+/Ca^{2+} exchange inhibitor KB-R7943 using the following experimental paradigm. In whole-cell voltage clamp mode, at a holding potential of −40 to −50 mV, AgOR/Orco mediated currents were initially activated by the respective odorant at a saturating concentration (100 μM). The drug was applied after the odorant-evoked currents reached a steady state level. KB-R7943 suppressed these currents in concentration-dependent manner (Fig. 2A and B). The KB-R7943 effects were partially irreversible with the degree of recovery depending on the concentration and exposure time to KB-R7943 (Fig. 2A inset, see also Figs. 3 and 4). The effects were strongly voltage dependent and were more pronounced in the positive voltage range (Fig. 2A and B). In some cases, high KB-R7943 concentrations augmented the inward currents (Fig. 2A and B). While interesting, the nature of these currents is difficult to interpret in terms of the standard/typical channel-blocker interaction. It should be noted however that KB-R7943 had little, if any, effect on either whole-cell currents of the cells expressing ORs in the absence of the respective ligands (n = 4/5) or on currents of untransfected HEK293T cells (n = 8). Overall the parameters of inhibition calculated from the KB-R7943 concentration dependences generated at ~+100 mV were (inhibition constant, IC_{50}; Hill coefficient, h; number of trials, n): for the AgOR48/AgOrco complex (18 ± 1.2, 1.2 ± 0.7, n = 6); for the AgOR65/AgOrco complex (14.1 ± 7.5, 1.2 ± 0.8, n = 3–6) (Fig. 2A and B). These results demonstrate that KB-R7943 is a potent inhibitor of insect ORs.

VUAA1 is a compound initially identified in a broad scale high throughput screening [7] to act as an agonist targeting the Orco subunit. We next tested whether KB-R7943 could block currents evoked by VUAA1 in a manner similar to which it blocks odorant-induced currents. As in the case of the cognate ligands, VUAA1 (100 μM) evoked currents were blocked by a saturating KB-R7943 concentration (100 μM, Fig. 3) and the KB-R7943 effects were partially irreversible (Fig. 3B, middle).

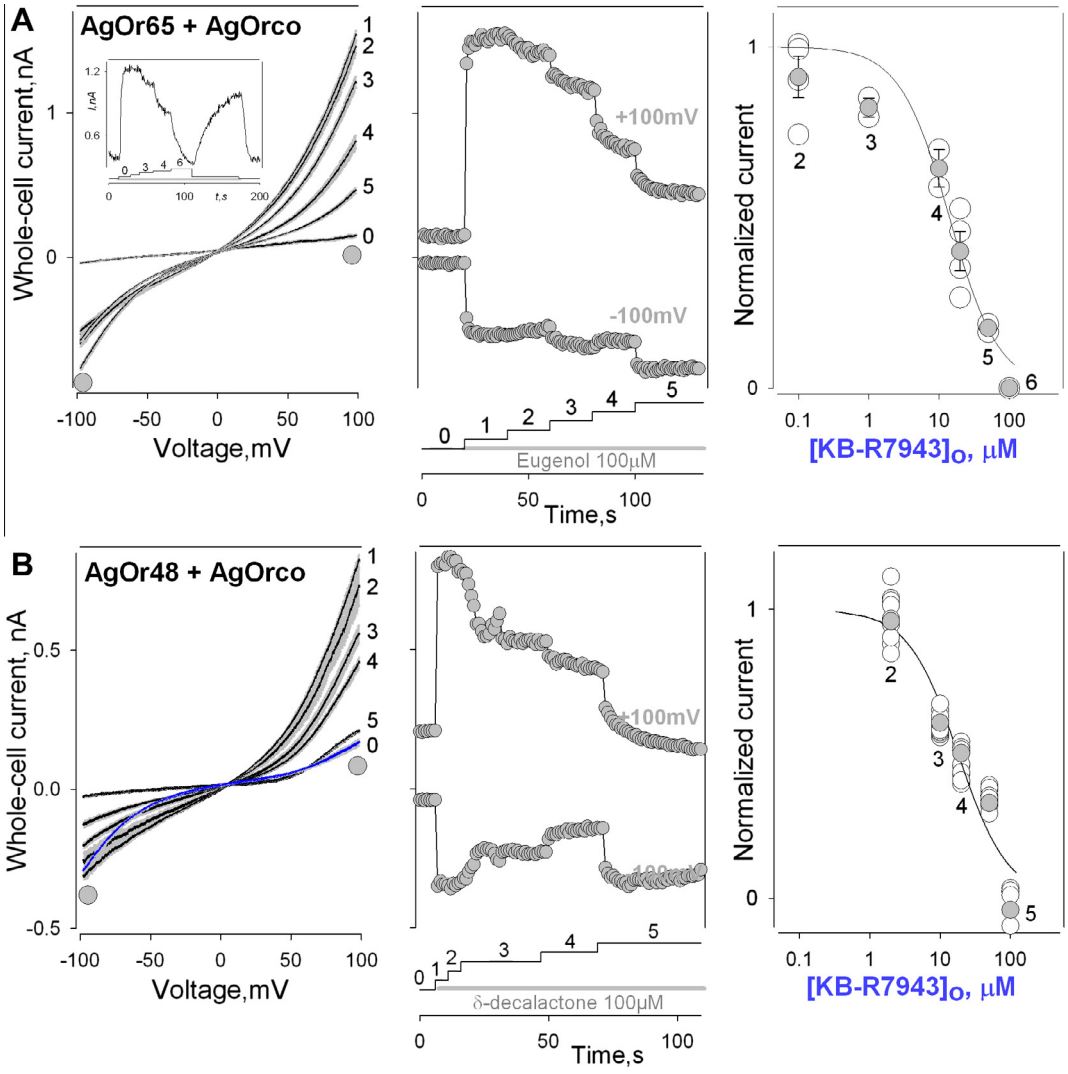

Fig. 2. Effects of KB-R7943 on odorant evoked AgOr mediated currents. KB-R7943 suppresses eugenol (100 μM) or δ-decalactone (100 μM) activated currents mediated by heteromeric AgOr65/AgOrco (A) or AgOr48/AgOrco (B) complexes heterologously expressed in HEK293T cells. Lefts panels – series of current voltage characteristics obtained in control condition and in the presence of different [KB-R7943] (curve index – μM): 1–0, 2–0.1, 3–1, 4–10, 5–50, 6–100. Current voltage dependences were obtained using a 15 ms duration voltage pulse to −100 mV followed by a 150 ms linear voltage change (ramp) to 100 mV. Only averaged traces ± respective SD ranges (gray color) are shown. Leak current subtraction and/or series resistance compensation were not applied. Holding potential was −50 mV. Time between sweep starts was 1 s. Middle panels – time course of the KB-R7943 effects. The current values were obtained from current–voltage curves (left panels, respective regions marked by symbols). Inset (A, left) shows that the KB-R7943 effects were at least partially reversible. Gap free current recording was obtained from the same cell. Holding potential was 50 mV. Data in Left and Middle panels were obtained from the same cells and have the same current scales. Diagrams at the bottom of the panels depict time course of different [KB-R7943] application. Note, effects of the drug are pronouncedly voltage dependent especially at high concentrations. Right panels – concentration dependencies of KB-R7943. Data were obtained at 100 mV. Normalized current mean values (gray circles) were fitted by a modification of the Hill equation with following parameters: for AgOr65/AgOrco $h \sim 1.2$, IC50 ~ 14.1 μM; for AgOr48/AgOrco $h \sim 1.2$, IC50 ~ 18 μM. (For interpretation of the references to color in this figure legend, the reader is referred to the web version of this article.)

We also tested the effects of KB-R7943 on VUAA1-evoked AgOR/Orco channel activity using outside-out membrane patch recordings. KB-R7943 applied to extracellular side of membrane patch reversibly inhibited VUAA1 activated channel currents (Fig. 3E and F, right panels). In some cases, the membrane patch current level recorded in the presence of 100 μM KB-R7943 was lower than the current noise in control conditions (before agonist application), perhaps suggesting some basal activity of AgORs. The channels demonstrated very brief gating parameters, opening and shutting events, making it practically impossible to carry out a detailed analysis of the gating behavior at the single channel level. While the outside out patch clamp recordings of single channel currents suggest that there is likely a direct interaction between KB-R7943 and AgORs, they provide little insight about the molecular target/mechanisms of the KB-R7943 effects. For example, it is still unclear whether inhibition is caused by an increased closed time of the channel (decrease in open channel probability) or by an open state block. Different approaches will be needed to address these questions in subsequent research.

When expressed in the absence of a ligand-specific subunit, AgOrco subunits form functional homomeric channels that can be activated by VUAA1 and VUAA1 related compounds [7,27]. We tested whether KB-R7943 was capable of blocking VUAA1-evoked currents in the cells expressing exclusively AgOrco and once again found that it could, with the effects of the blocker were only partially reversible and appeared to be voltage independent (Fig. 4A). The parameters of inhibition were estimated to be $[KB\text{-}R7943]_{1/2}$ ~5.4 μM, $h \sim 1.6$, $n = 3–7$ (Fig. 4A, right panel). Since KB-R7943 has an effect independent of expression of the ligand-specific subunits, these results suggest that the Orco subunit or

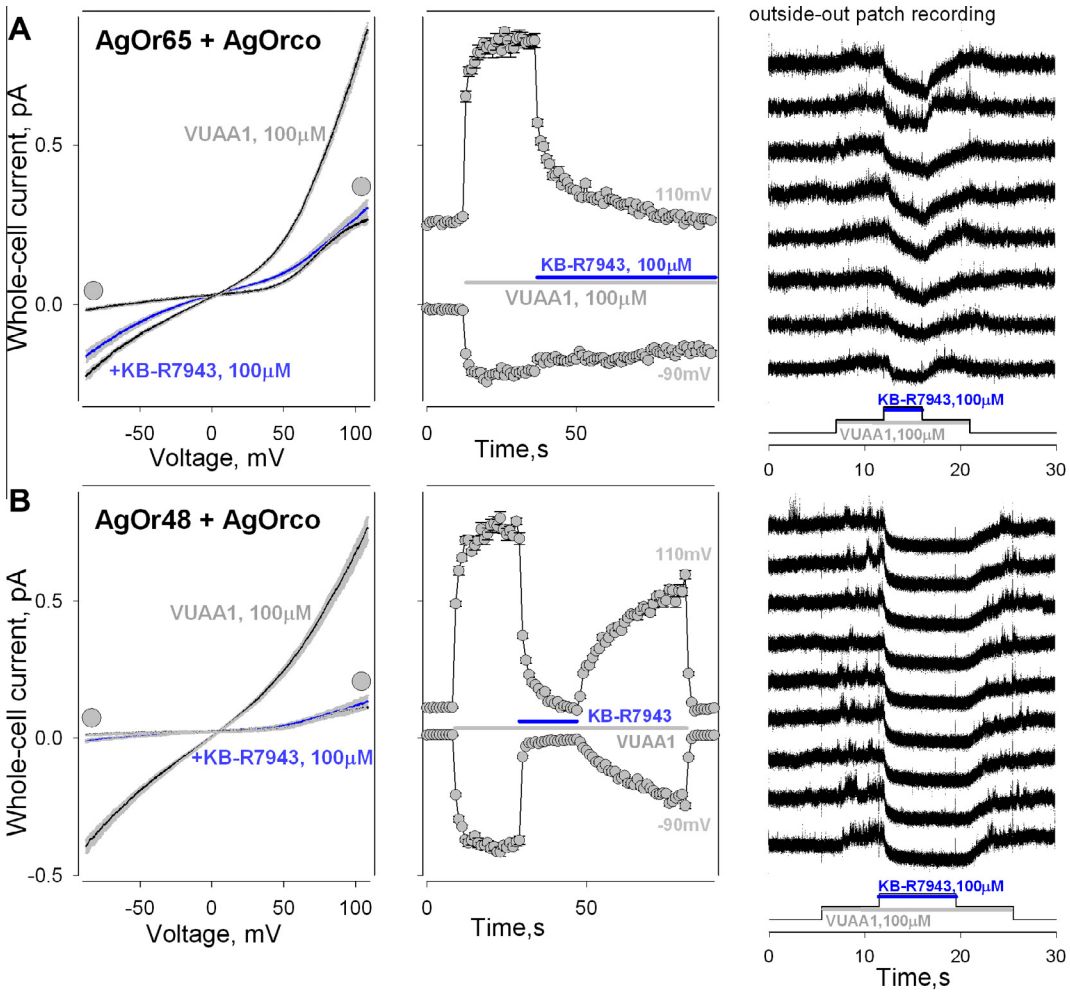

Fig. 3. Effects of KB-R7943 on VUAA1 evoked AgOr mediated currents. KB-R7943 suppresses VUAA1 activated currents mediated by heteromeric AgOr65/AgOrco (A) or AgOr48/AgOrco (B) complexes. Lefts panels – series of current–voltage characteristics obtained under control conditions and in the presence of KB-R7943 100 μM. Current–voltage dependences were obtained using a 15 ms duration voltage pulse to −90 mV followed by a 150 ms linear voltage change (ramp) to 110 mV. Only averaged traces ± respective SD ranges (gray color) are shown. Leak current subtraction and/or series resistance compensation were not applied. Holding potential was −40 mV. Time between sweep starts was 1 s. Middle panels – time course of the KB-R7943 effects. The current values were obtained from current–voltage curves (left panels, respective regions marked by symbols). Data in Left and Middle panels were obtained from the same cells and have the same current scales. Bars in the panels depict time course of VUAA1 and KB-R7943 application. Note, voltage dependence of drug effects is not pronounced in case of AgOr48/AgOrco. Right panels – examples of outside-out patch recordings. AgOr65/AgOrco and AgOr48/AgOrco complexes were activated by the nonspecific agonist VUAA1 followed by reversible inhibition by application of KB-R7943 100 μM. Note, increased current noise evoked by VUAA1 was interpreted as an increase in channel activity. Unitary currents are not distinguishable likely due to flickery gating and low single channel conductance. (For interpretation of the references to color in this figure legend, the reader is referred to the web version of this article.)

an associated protein endogenous to the HEK293T cells may be the target of the drug's action. Interestingly, the effects of KB-R794 on VUAA1 activated currents recorded from cells expressing AgOr48 + AgOrco or AgOrco alone were significantly less voltage dependent in comparison to cells expressing AgOr65 + AgOrco (compare Fig. 3B, Fig. 4A and Fig. 3A). While speculative in the context of the current report these differences could be explained by variations in the biophysical and pharmacological characteristics of the receptor channel complexes predetermined by interaction of particular ligand-specific subunits with Orco [28–30].

Given that the blocking efficiency of KB-R7943 on currents generated by the cells expressing heteromeric AgOR/Orco complexes and activated by their cognate ligands is considerably voltage dependent, we next used calcium imaging to determine if KB-R7943 could be effective in "intact" (uncontrolled) voltage conditions. As in the electrophysiological experiments, KB-R7943 application suppressed calcium influx evoked by both the cognate ligands δ-decalactone (1–50 μM) and eugenol (1–50 μM) as well as that evoked by VUAA1 (50 μM) (Fig. 4B). The KB-R7943 effects were irreversible (only partially reversible after ~20–30 min washout), which made it impractical to determine the concentration dependence of the blockade. Under these experimental conditions, KB-R7943 was considerably more potent in that incubation with even 10 μM KB-R7943 almost completely blocked the calcium responses. However, it is important to note that we cannot exclude the possibility that the compound can accumulate within cells or the cell membrane fraction ($\mathrm{Log}P \sim 2.87$, estimated using Advanced Chemistry Development (ACD/Labs) Software V11.02), thereby shifting the apparent inhibition constant. The different calcium response kinetics (calcium signal decay time is noticeably slower for AgOr48 + AgOrco, Fig. 4B) are likely due to the differences in extracellular divalent cation concentrations used in the experiments. Overall despite the different experimental approach and experimental conditions, KB-R7943 was able to effectively disrupt both odorant and VUAA1 evoked calcium signals, consistent with data obtained in electrophysiological experiments.

The shared sensitivity of HEK293T cells expressing insect ORs and lobster ORNs expressing IRs to the pharmacological blockers

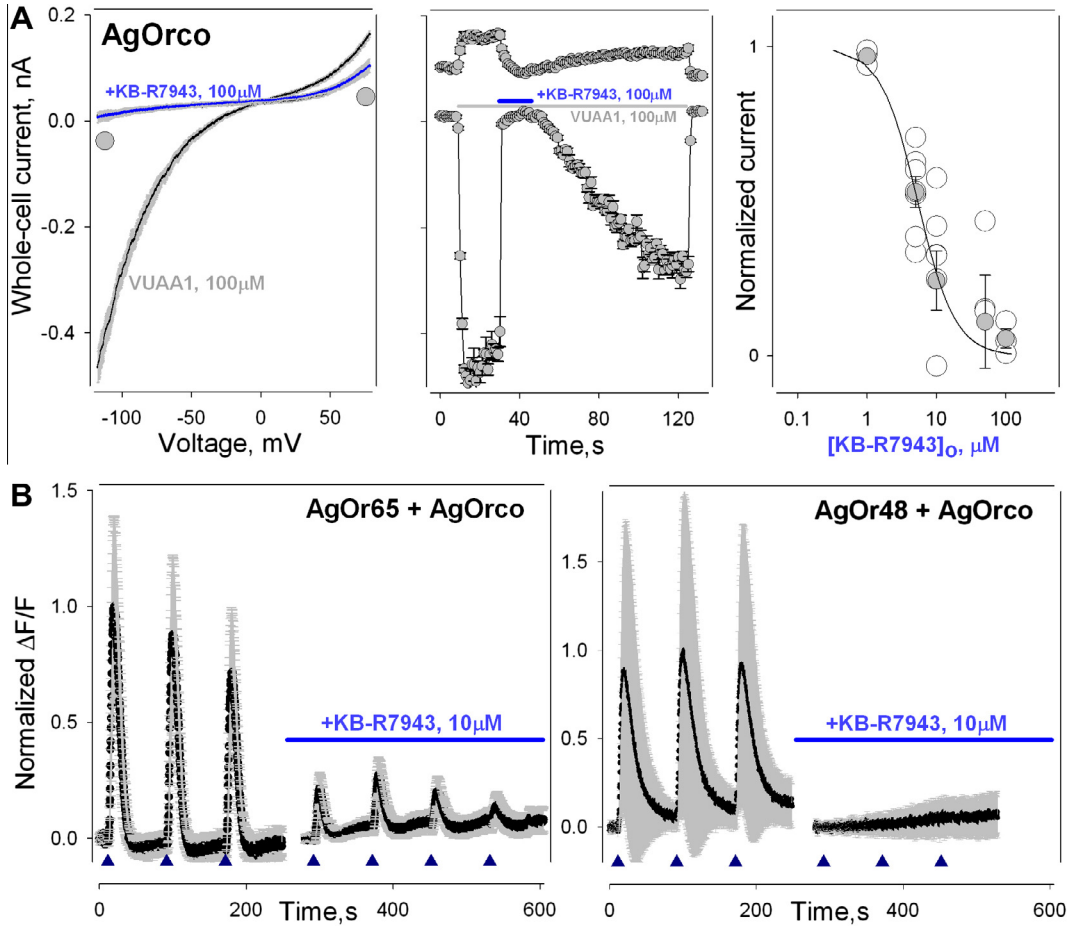

Fig. 4. Effects of KB-R7943 on VUAA1 evoked AgOrco mediated currents. (A) KB-R7943 suppresses VUAA1 activated currents mediated by homomeric AgOrco complexes. Lefts panel – Current–voltage characteristics obtained under control conditions and in the presence of KB-R7943 100 μM. Current–voltage dependences were recorded using a 15 ms duration voltage pulse to −120 mV followed by a 150 ms linear voltage change (ramp) to 80 mV. Only averaged traces ± respective SD ranges (gray color) are shown. Holding potential was −70 mV. Time between sweep starts was 1 s. Middle panel – time course of the KB-R7943 effects. The current values were obtained from current–voltage curves (left panels, respective regions marked by symbols). Data in Left and Middle panel were obtained from the same cell and have the same current scales. Right panel – concentration dependencies of KB-R7943. Data were obtained at 80 mV. Normalized current mean values (gray circles) were fitted by a modification of the Hill equation with following parameters: $h \sim 1.6$, IC50~5.4 μM. Bars in the panels depict time course of VUAA1 and KB-R7943 application. (B) KB-R7943 blocks the stimulus evoked calcium signal in HEK cells expressing either AgOr65/AgOrco (left) or AgOr48/AgOrco (right) complexes. AgOr65/AgOrco expressing cells were stimulated with 50 μM VUAA1 while AgOr48/AgOrco cells were stimulated with 10 μM δ-decalactone. AgOr48/AgOrco expressing cells were incubated in the solution containing 2 mM Ca^{2+}, 0 Mg^{2+}. Triangles and bars in the panels depict the time course of the stimulus (5 s pulse duration was used in all cases) and KB-R7943 application. (For interpretation of the references to color in this figure legend, the reader is referred to the web version of this article.)

including KB-R7943 [9,10,31,17] provides further support for that idea that these structurally different types of arthropod ionotropic chemosensory receptors are functionally similar. It also raises the specter of a novel functional mechanism – co-assembly of olfactory receptors with a ubiquitously expressed, conserved ion transporter. This idea gains support from the recent finding that ion channels and ion exchangers can form integral supra-molecular complexes with reciprocal pharmacology [32–37] and provides a new target for compounds designed to improve control of insect pests and disease vectors. Towards that end, we hope that our findings will stimulate a larger scale pharmacological and molecular analysis to identify and functionally characterize potential OR/IR-ion transporter/exchanger interactions.

Acknowledgments

This work was supported by National Institute on Deafness and Other Communication Disorders (DC001655). We thank Dr. Larry Zwiebel for generously sharing HEK cell lines expressing the mosquito OR complexes and VUAA1.

References

[1] K. Sato, M. Pellegrino, T. Nakagawa, T. Nakagawa, L.B. Vosshall, K. Touhara, Insect olfactory receptors are heteromeric ligand-gated ion channels, Nature 452 (2008) 1002–1009.
[2] D. Wicher, R. Schafer, R. Bauernfeind, M.C. Stensmyr, R. Heller, S.H. Heinemann, B.S. Hansson, Drosophila odorant receptors are both ligand-gated and cyclic-nucleotide-activated cation channels, Nature 452 (2008) 1007–1010.
[3] K. Sato, K. Tanaka, K. Touhara, Sugar-regulated cation channel formed by an insect gustatory receptor, Proc. Natl. Acad. Sci. U.S.A. 108 (2011) 11680–11685.
[4] E.G. Freeman, Z. Wisotsky, A. Dahanukar, Detection of sweet tastants by a conserved group of insect gustatory receptors, Proc. Natl. Acad. Sci. U.S.A. 111 (2014) 1598–1603.
[5] R. Benton, K.S. Vannice, C. Gomez-Diaz, L.B. Vosshall, Variant ionotropic glutamate receptors as chemosensory receptors in Drosophila, Cell 136 (2009) 149–162.
[6] L. Abuin, B. Bargeton, M.H. Ulbrich, E.Y. Isacoff, S. Kellenberger, R. Benton, Functional architecture of olfactory ionotropic glutamate receptors, Neuron 69 (2011) 44–60.
[7] P.L. Jones, G.M. Pask, D.C. Rinker, L.J. Zwiebel, Functional agonism of insect odorant receptor ion channels, Proc. Natl. Acad. Sci. U.S.A. 108 (2011) 8821–8825.
[8] T. Nakagawa, T. Sakurai, T. Nishioka, K. Touhara, Insect sex-pheromone signals mediated by specific combinations of olfactory receptors, Science 307 (2005) 1638–1642.

[9] G.M. Pask, Y.V. Bobkov, E.A. Corey, B.W. Ache, L.J. Zwiebel, Blockade of insect odorant receptor currents by amiloride derivatives, Chem. Senses 38 (2013) 221–229.
[10] K. Roellecke, M. Werner, P.M. Ziemba, E.M. Neuhaus, H. Hatt, G. Gisselmann, Amiloride derivatives are effective blockers of insect odorant receptors, Chem. Senses 38 (2013) 231–236.
[11] T.R. Kleyman, E.J. Cragoe, Amiloride and its analogs as tools in the study of ion-transport, J. Membr. Biol. 105 (1988) 1–21.
[12] F. Rogister, D. Laeckmann, P.O. Plasman, F. Van Eylen, M. Ghyoot, C. Maggetto, J.F. Liegeois, J. Geczy, A. Herchuelz, J. Delarge, B. Masereel, Novel inhibitors of the sodium-calcium exchanger: benzene ring analogues of *N*-guanidino substituted amiloride derivatives, Eur. J. Med. Chem. 36 (2001) 597–614.
[13] M.P. Blaustein, W.J. Lederer, Sodium calcium exchange: its physiological implications, Physiol. Rev. 79 (1999) 763–854.
[14] H.L. Ji, R.Z. Zhao, Z.X. Chen, S. Shetty, S. Idell, S. Matalon, Delta ENaC: a novel divergent amiloride-inhibitable sodium channel, Am. J. Physiol. Lung Cell Mol. Physiol. 303 (2012) L1013–L1026.
[15] T. Iwamoto, T. Watano, M. Shigekawa, A novel isothiourea derivative selectively inhibits the reverse mode of Na^+/Ca^{2+} exchange in cells expressing NCX1, J. Biol. Chem. 271 (1996) 22391–22397.
[16] T. Watano, J. Kimura, T. Morita, H. Nakanishi, A novel antagonist, No. 7943, of the Na^+/Ca^{2+} exchange current in guinea-pig cardiac ventricular cells, Br. J. Pharmacol. 119 (1996) 555–563.
[17] A. Pezier, Y. Bobkov, V.B. Ache, The Na^+/Ca^{2+} exchanger inhibitor, KB-R7943, blocks a nonselective cation channel implicated in chemosensory transduction, J. Neurophysiol. 101 (2009) 1151–1159.
[18] B. Hollins, D. Hardin, A.A. Gimelbrant, T.S. Mcclintock, Olfactory-enriched transcripts are cell-specific markers in the lobster olfactory organ, J. Comp. Neurol. 455 (2003) 125–138.
[19] E.A. Corey, Y. Bobkov, K. Ukhanov, B.W. Ache, Ionotropic crustacean olfactory receptors, PLoS ONE 8 (2013).
[20] J.D. Bohbot, P.L. Jones, G. Wang, R. Pitts, G.M. Pask, L.J. Zwiebel, Conservation of indole responsive odorant receptors in mosquitoes reveals an ancient olfactory trait, Chem. Senses 36 (2011) 149–160.
[21] P. Kain, T.S. Chakraborty, S. Sundaram, O. Siddiqi, V. Rodrigues, G. Hasan, Reduced odor responses from antennal neurons of G(q)alpha, phospholipase C beta, and rdgA mutants in Drosophila support a role for a phospholipid intermediate in insect olfactory transduction, J. Neurosci. 28 (2008) 4745–4755.
[22] Y.D. Deng, W.Y. Zhang, K. Farhat, S. Oberland, G. Gisselmann, E.M. Neuhaus, The stimulatory G alpha(s) protein is involved in olfactory signal transduction in Drosophila, PLoS ONE 6 (2011).
[23] A. Nolte, N.W. Funk, L. Mukunda, P. Gawalek, A. Werckenthin, B.S. Hansson, D. Wicher, M. Stengl, In situ tip-recordings found no evidence for an Orco-based ionotropic mechanism of pheromone-transduction in *Manduca sexta*, PLoS ONE 8 (2013).
[24] J.S. Ignatious Raja, N. Katanayeva, V.L. Katanaev, C.G. Galizia, Role of Go/i subgroup of G proteins in olfactory signaling of *Drosophila melanogasteri*, Eur. J. Neurosci. 39 (2014) 1245–1255.
[25] R.F. Mitchell, D.T. Hughes, C.W. Luetje, J.G. Millar, F. Soriano-Agaton, L.M. Hanks, H.M. Robertson, Sequencing and characterizing odorant receptors of the cerambycid beetle *Megacyllene caryae*, Insect Biochem. Mol. Biol. 42 (2012) 499–505.
[26] P.X. Xu, Y.M. Choo, J. Pelletier, F.R. Sujimoto, D.T. Hughes, F. Zhu, E. Atungulu, A.J. Cornel, C.W. Luetje, W.S. Leal, Silent, generic and plant kairomone sensitive odorant receptors from the Southern house mosquito, J. Insect Physiol. 59 (2013) 961–966.
[27] S.S. Chen, C.W. Luetje, Identification of new agonists and antagonists of the insect odorant receptor co-receptor subunit, PLoS ONE 7 (2012).
[28] A.S. Nichols, S.S. Chen, C.W. Luetje, Subunit contributions to insect olfactory receptor function: channel block and odorant recognition, Chem. Senses 36 (2011) 781–790.
[29] G.M. Pask, P.L. Jones, M. Ruetzler, D.C. Rinker, L.J. Zwiebel, Heteromeric anopheline odorant receptors exhibit distinct channel properties, PLoS ONE 6 (2011).
[30] T. Nakagawa, M. Pellegrino, K. Sato, L.B. Vosshall, K. Touhara, Amino acid residues contributing to function of the heteromeric insect olfactory receptor complex, PLoS ONE 7 (2012).
[31] Y.V. Bobkov, B.W. Ache, Block by amiloride derivatives of odor-evoked discharge in lobster olfactory receptor neurons through action on a presumptive TRP channel, Chem. Senses 32 (2007) 149–159.
[32] A. Schwarzer, H. Schauf, P.J. Bauer, Binding of the cGMP-gated channel to the Na/Ca-K exchanger in rod photoreceptors, J. Biol. Chem. 275 (2000) 13448–13454.
[33] A. Poetsch, L.L. Molday, R.S. Molday, The cGMP-gated channel and related glutamic acid-rich proteins interact with peripherin-2 at the rim region of rod photoreceptor disc membranes, J. Biol. Chem. 276 (2001) 48009–48016.
[34] K. Kang, P.J. Bauer, T.G. Kinjo, R.T. Szerencsei, W. Bonigk, R.J. Winkfein, P.P.M. Schnetkamp, Assembly of retinal rod or cone Na^+/Ca^{2+}-K^+ exchanger oligomers with cGMP-gated channel subunits as probed with heterologously expressed CDNAs, Biochemistry 42 (2003) 4593–4600.
[35] C. Rosker, A. Graziani, M. Lukas, P. Eder, M.X. Zhu, C. Romanin, K. Groschner, Ca^{2+} signaling by TRPC3 involves Na^+ entry and local coupling to the Na^+/Ca^{2+} exchanger, J. Biol. Chem. 279 (2004) 13696–13704.
[36] P. Eder, D. Probst, C. Rosker, M. Poteser, H. Wolinski, S. Kohwein, C. Romanin, K. Groschner, Phospholipase C-dependent control of cardiac calcium homeostasis involves a TRPC3-NCX1 signaling complex, Cardiovasc. Res. 73 (2007) 111–119.
[37] L.M. Louhivuori, L. Jansson, T. Nordstrom, G. Bart, J. Nasman, K.E. Akerman, Selective interference with TRPC3/6 channels disrupts OX1 receptor signalling via NCX and reveals a distinct calcium influx pathway, Cell Calcium 48 (2010) 114–123.